Available online at http://scik.org

Commun. Math. Biol. Neurosci. 2024, 2024:133

https://doi.org/10.28919/cmbn/8930

ISSN: 2052-2541

MATHEMATICAL STOCHASTICS MODEL OF TUBERCULOSIS USING EMPIRICAL DATA FROM MALANG CITY

LUKMAN HAKIM[1,*], IESYAH RODLIYAH[2]

Department of Computer Science, Faculty of Technology and Design, Institut Teknologi dan Bisnis Asia, Malang, East Java, Indonesia

Department of Mathematics Education, Faculty of Education, Universitas Hasyim Asy'ari Tebuireng, Jombang, East Java, Indonesia

Abstract: Mathematical models are utilized as a powerful tool to describe the transmission of diseases, especially Tuberculosis. Throughout these models, differential equations systems are commonly implemented. In this study employs a nonlinear differential equation to portray the disease of Tuberculosis, and the model was constructed in deterministic and stochastic systems. According to the deterministic model, we elaborate the positivity and boundedness of solutions, then two fixed points were obtained, which are disease-free equilibrium and endemic equilibrium points, and their stability conditions is established using Routh Hurwitz. Furthermore, the reproduction number is found by demonstrating the maximum of eigen value utilizing the next-generation matrix. Further discussion related to constructing a deterministic model involving two control variables, i.e. an effort to maintain distance between the susceptible population and the infected population, and efforts to treat the infected population. Analysis of optimal control problems by using the Pontryagin principle. Last study establishes about numerical simulations and parameter estimation using genetic algorithms. Both deterministic and stochastic models rely on parameter estimate results for simulation. Applying different disturbance levels to the stochastic model has a significant impact on the dynamical solution. In accordance to the optimal control simulation, the second control variable performs better than the first.

Keywords: tuberculosis; deterministic; stochastic; local stability; optimal control; Malang city.

2020 AMS Subject Classification: 34A12, 49J30, 92D25, 93A30.

*Corresponding author

E-mail address: bledeklukman@gmail.com

Received September 30, 2024

1. INTRODUCTION

Tuberculosis is a contagious disease caused by Mycobacterium, affecting organs beyond the respiratory system. Tuberculosis is a significant worldwide public health concern, especially in countries with limited medical resources. The World Health Organization indicates that tuberculosis is the foremost cause of death from infectious diseases worldwide, behind HIV/AIDS. The WHO projected that in 2020, there were over 10 million new tuberculosis infections and 1.5 million deaths. The incidence of TB varies by nation, with elevated infection rates in particular among countries with low or middle incomes., such as South Asia, Sub-Saharan Africa, and some parts of Eastern Europe [1], [2].

Tuberculosis is transmitted by airborne droplets when an infected person coughs or sneezes. This droplet contains bacteria and may be breathed by others. Upon entering the lungs, tuberculosis bacteria may remain latent for several times before presenting as active disease, especially in individuals with weakness immune, such as those with HIV, diabetes, and malnutrition [3]. Pulmonary TB is the primary form of tuberculosis disease. The principal symptoms are a persistent at lasting over three weeks, fever, night sweats, and considerable weight loss. In extrapulmonary tuberculosis, symptoms vary depending on the affected organ, including bones, and the genitourinary system.

Tuberculosis is a global epidemic that poses a substantial concern, being the primary cause of mortality in several regions worldwide. Based on the 2023 edition of the Global Tuberculosis Report, WHO has declared tuberculosis an emerging disease because over 99% of the world's population has reported cases of tuberculosis [2]. Indonesia recorded a mortality incidence of 14% in 2022, and Indonesia reported the highest number of TB cases in 2023, totaling 809,000. Focusing on Malang City, and referring to the Health Profile of Malang City in 2022, the Health Office reported a suspected tuberculosis case until 17.010, with 1.632 cases detected positive for TB in hospitals, 565 cases in community health centers, and 19 cases in other institutions [4].

Based on the background previously, there is an urgency to conduct future research on controlling and managing the TB pandemic. One of the control strategies that might be employed

is applicable to epidemiology by approaching mathematical model analysis [5]–[7] and numerical simulation [8], [9]. The research that examines the tuberculosis through modeling includes OJo et al. [10], and Madaki et al. (2020) studied the spread of TB with treatment concern [11]. Ucakan et al. (2021) analyzed tuberculosis in Turkey using a deterministic model, which indicated the effectiveness of vaccination [12]. Additionally, Mekonen et al. (2021) investigated the analysis of co-infection between tuberculosis and COVID-19 [13], further supported by findings of Inayaturohmat et al. [14]. Meanwhile, in 2022, the dynamics of TB spread modeled and analyzed by Sulayman and Abdullah [15], Kuddus et al. modeled TB cases in Bangladesh [16], and Avilov et al. conducted research demonstrating that active TB data could support assumptions for estimating the spreading of TB in Russia [3].

The research above illustrates a deterministic mathematical model, and the recent tuberculosis study by Oshinubi et al. (2023) using a deterministic fractional model, and showing that treatment method has a positive effect in controlling disease [17]. Furthermore, the combination of deterministic models and optimal control was studied by Xue et al. [18], and has been examined by Hakim (2022) as a technique for controlling measles [19], managing COVID-19 infections [20]–[22], and modeling diphtheria [23]. Hakim et al. used control theory for predicting cholera disease [24], which was also in line by Igoe et al. [25]. In 2023, Hakim derived the research about optimal control regarding the spread of COVID-19, by taking quarantine and vaccination policies [20]. In addition, several research on optimal control in tuberculosis through vaccination and treatment [26], and utilizing the vaccinated population and reinfection cases [27]. Other studies consider the vaccination process in the latent population, which is divided into two categories [28].

This research article is structured into many sections. The first section shows the context and related research about the transmission of diseases, with a particular focus on Tuberculosis. Secondly, outlines the biological assumptions and guidelines of deterministic and stochastic models with saturated infection. The third section discusses the analysis of the solution dynamics of the TB model, including positivity and boundedness properties, fixed points, basic reproduction number, and their stability condition. The fourth part breaks down the use of optimum control variables inside the deterministic tuberculosis model, along by an investigation of the optimal

control problem. Finally, this section examines the numerical simulations of deterministic models, stochastic models, and optimal control result.

2. CONSTRUCTION MODEL OF TUBERCULOSIS

Based on the biological assumptions, we constructed a mathematical model of Tuberculosis with saturation function [29] is $h(t) = \frac{1}{1+\eta I(t)}$. By following the previous assumptions, we get the deterministic system as

$$\begin{aligned}
\frac{dS(t)}{dt} &= \pi - \frac{\beta S(t)I(t)}{1+\eta I(t)} - \mu S(t) \\
\frac{dE(t)}{dt} &= \frac{\beta S(t)I(t)}{1+\eta I(t)} - (\mu+\nu)E(t) \\
\frac{dI(t)}{dt} &= \nu E(t) - (\gamma+\alpha+\mu)I(t) + \theta R(t) \\
\frac{dR(t)}{dt} &= \gamma I(t) - (\mu+\theta)R(t),
\end{aligned} \tag{1}$$

with the total population is $N(t) = S(t) + E(t) + I(t) + R(t)$. The variable $S(t)$ depicts the density of the susceptible subpopulation during time, namely those individuals at risk of infection. $E(t)$ represents a subpopulation infected by the Mycobacterium agent, which does not seem to provide a significant health risk and is recognized by the exposed populations. $I(t)$ represents the infected subpopulation, those expressing the dangerous illness and associated with symptoms in disease. Variable $R(t)$ denotes the number of the recovered subgroup. Then, a modification model (1) will be executed by adding the noise or disturbances, and it represent the stochastic behavior. Consequently, model (1) could be reformulated as a stochastic differential equation in the following:

$$\begin{aligned}
dS &= \left(\mu N - \frac{\beta SI}{1+\eta I} - \mu S\right)dt + \sigma_S S dW_s \\
dE &= \left(\frac{\beta SI}{1+\eta I} - (\mu+\nu)E\right)dt + \sigma_E E dW_E \\
dI &= (\nu E - (\gamma+\alpha+\mu)I)dt + \sigma_I I dW_I
\end{aligned} \tag{2}$$

$$dR = (\gamma I - \mu R)dt + \sigma_R R dW_R,$$

with the value $\sigma_S, \sigma_E, \sigma_I$, and σ_R are the perturbation (noise) variables, and W_s, W_E, W_I, W_R are Wiener process or Brownian process. The positive parameters of systems (1) are detailed in Table 1.

Table 1. Parameters Description

Parameters	Interpretation
π	A reproductive rate of susceptible
β	The contact rate of susceptible with infectious subgroup
η	The saturation rate of infection
μ	The natural mortality rate
ν	The rate of exposed become infected
α	The mortality cause infection
γ	Recovery rate
θ	Reinfection rate

3. ANALYSIS OF TUBERCULOSIS MODEL WITHOUT NOISE AND THEIR PROPERTIES

3.1 POSITIVITY AND BOUNDEDNESS CONDITION OF SOLUTION

In this section, we will declare that the solutions of model (1) are non-negative and bounded, as well as that the model is most influential and meaningful.

Theorem 1. *By respecting to the model (1), the set W is the invariant manifold, and it is finally bounded.*

Proof. All populations $N(t) = S(t) + E(t) + I(t) + R(t)$, and it is becoming

$$\frac{dN(t)}{dt} = \frac{dS(t)}{dt} + \frac{dE(t)}{dt} + \frac{dI(t)}{dt} + \frac{dR(t)}{dt}. \tag{3}$$

Then, by substituting equations (1) into equation (3) gives

$$\begin{aligned}\frac{dN(t)}{dt} = \pi - \frac{\beta S(t)I(t)}{1+\eta I(t)} - \mu S(t) + \frac{\beta S(t)I(t)}{1+\eta I(t)} - (\mu+\nu)E(t) + \nu E(t) \\ - (\gamma + \alpha + \mu)I(t) + \theta R(t) + \gamma I(t) - (\mu+\theta)R(t).\end{aligned} \tag{4}$$

Through the application of basic algebraic, we derive

$$\frac{dN(t)}{dt} = \pi - \mu\big(S(t) + E(t) + I(t) + R(t)\big). \tag{5}$$

hence $S(t) + E(t) + I(t) + R(t) = N(t)$, then we have

$$\frac{dN(t)}{dt} = \pi - \mu N(t). \tag{6}$$

Upon rewriting equation (6), we represent the first-order linear ordinary differential equation below

$$\frac{dN(t)}{dt} + \mu N(t) = \pi,$$

and by integrating factors, we get the trivial solution is

$$N(t) = \frac{\pi}{\mu} + Ke^{-\mu t}, \tag{7}$$

with K is constant. By taking $t = 0$, we have the solution of initial value is $N(0) = \frac{\pi}{\mu} + K$. Therefore,

$$K = N(0) - \frac{\pi}{\mu}. \tag{8}$$

Applying the value of K in equation (8) into equation (7), then the solutions with the initial condition can be stated with

$$N(t) = \frac{\pi}{\mu} + \left(N(0) - \frac{\pi}{\mu}\right) e^{-\mu t}. \tag{9}$$

It is visible that $\lim_{t\to\infty} N(t) = \frac{\pi}{\mu}$, and thus $N(t)$ is bounded with value $\frac{\pi}{\mu}$. Consequently, we can verify that all solutions to equation (1) in line on the field

$$\mathcal{W} = \left\{(S, E, I, R) \in \mathbb{R}_+^4 : 0 \le N \le \frac{\pi}{\mu}\right\},$$

with $S(0), E(0), I(0), R(0) \in \mathcal{W}$. ⊡

Theorem 2. *All Positive values are obtained on the solutions of equation (1) if the initial conditions* $S(0), E(0), I(0), R(0) \ge 0 \in W$.

Proof. It is readily obvious that all solutions of equation (1) are non-negative values,

$$\left.\frac{dS(t)}{dt}\right|_{S=0} = \pi > 0,$$

$$\left.\frac{dE(t)}{dt}\right|_{E=0} = \frac{\beta S(t) I(t)}{1 + \eta I(t)} \ge 0,$$

$$\left.\frac{dI(t)}{dt}\right|_{I=0} = \nu E(t) + \theta R(t) \geq 0,$$

$$\left.\frac{dR(t)}{dt}\right|_{R=0} = \gamma I(t) \geq 0,$$

it strengthens all findings into positive values. ⊡

3.2 EQUILIBRIUM POITS

The equilibrium point is achieved when $\frac{dS(t)}{dt} = \frac{dE(t)}{dt} = \frac{dI(t)}{dt} = \frac{dR(t)}{dt} = 0$. The disease-free equilibrium point is the condition in which the disease has been eradicated or no pandemic, signifying that $I(t) = 0$. By using the value $I(t) = 0$, we have the explicitly of susceptible subpopulation as

$$\frac{dS(t)}{dt} = \pi - \mu S(t), \tag{10}$$

and the equilibrium point is obtained through $\frac{dS(t)}{dt} = 0$, then we rewrite

$$0 = \pi - \mu S(t). \tag{11}$$

From (11), the trivial solution is obtained

$$S(t) = \frac{\pi}{\mu}. \tag{12}$$

Then we derive the new expression of exposed equations

$$\frac{dE(t)}{dt} = -(\mu + \nu)E(t), \tag{13}$$

As a result, the value of $E(t) = 0$. It is then clear that the value of $R(t) = 0$. Thus, the disease-free equilibrium point is $E_0(S, E, I, R) = \left(\frac{\pi}{\mu}, 0,0,0\right)$. Utilizing a disease-free fixed point, we can figure out the fundamental reproduction number or a threshold value indicative of a pandemic's existence. The fundamental reproduction number can possibly be derived from the next generation matrix (NGM) [29], namely

$$K = FV^{-1}, \tag{14}$$

with F is the transmission matrix and V is the transition matrix of a disease model. Next step, we assume that

$$\begin{bmatrix} f_1 \\ f_2 \end{bmatrix} = \begin{bmatrix} \dfrac{\beta SI}{1+\eta I} \\ \nu E + \theta R \end{bmatrix},$$

and

$$\begin{bmatrix} v_1 \\ v_2 \end{bmatrix} = \begin{bmatrix} -(\mu+\nu)E \\ -(\gamma+\alpha+\mu)I \end{bmatrix}.$$

Therefore, matrices F and V become Jacobian matrices expressed as follows,

$$F = \begin{bmatrix} \dfrac{\partial f_1}{\partial E} & \dfrac{\partial f_1}{\partial I} \\ \dfrac{\partial f_2}{\partial E} & \dfrac{\partial f_2}{\partial I} \end{bmatrix} = \begin{bmatrix} 0 & \dfrac{\beta S}{(1+\eta I)^2} \\ \nu & 0 \end{bmatrix},$$

and

$$V = \begin{bmatrix} \dfrac{\partial v_1}{\partial E} & \dfrac{\partial v_1}{\partial I} \\ \dfrac{\partial v_2}{\partial E} & \dfrac{\partial v_2}{\partial I} \end{bmatrix} = \begin{bmatrix} -(\mu+\nu) & 0 \\ 0 & -(\gamma+\alpha+\mu) \end{bmatrix}.$$

Substituting the disease-free fixed point into the matrices F and V produces

$$F = \begin{bmatrix} 0 & \dfrac{\beta\pi}{\mu} \\ \nu & 0 \end{bmatrix},$$

and

$$V = \begin{bmatrix} -(\mu+\nu) & 0 \\ 0 & -(\gamma+\alpha+\mu) \end{bmatrix}.$$

Then determine the inverse of matrix V, which is

$$V^{-1} = \frac{1}{(\gamma+\alpha+\mu)(\mu+\nu)} \begin{bmatrix} -(\gamma+\alpha+\mu) & 0 \\ 0 & -(\mu+\nu) \end{bmatrix} = \begin{bmatrix} -\dfrac{1}{(\mu+\nu)} & 0 \\ 0 & -\dfrac{1}{(\gamma+\alpha+\mu)} \end{bmatrix}.$$

Determine the equation (14), we evaluate the value of K as follows

$$K = FV^{-1} = \begin{bmatrix} 0 & \dfrac{\beta\pi}{\mu} \\ \nu & 0 \end{bmatrix} \begin{bmatrix} -\dfrac{1}{(\mu+\nu)} & 0 \\ 0 & -\dfrac{1}{(\gamma+\alpha+\mu)} \end{bmatrix} = \begin{bmatrix} 0 & -\dfrac{\beta\pi}{\mu(\gamma+\alpha+\mu)} \\ -\dfrac{\nu}{(\mu+\nu)} & 0 \end{bmatrix}.$$

Moreover, the basic reproduction number represents the greatest eigenvalue of matrix K trough the characteristic equation bellow

$$\lambda^2 - \frac{\beta\pi\nu}{\mu(\mu+\nu)(\gamma+\alpha+\mu)} = 0.$$

Finally, the value of reproduction number R_0 is

$$R_0 = \max\left(-\sqrt{\frac{\beta\pi\nu}{\mu(\mu+\nu)(\gamma+\alpha+\mu)}}, \sqrt{\frac{\beta\pi\nu}{\mu(\mu+\nu)(\gamma+\alpha+\mu)}}\right) = \sqrt{\frac{\beta\pi\nu}{\mu(\mu+\nu)(\gamma+\alpha+\mu)}}.$$

Alongside the disease-free equilibrium point, there exists an endemic equilibrium point, characterized by the disease's spreading throughout different places, indicating $I(t) \neq 0$. During algebraic analysis, the endemic equilibrium point $E^* = (S^*(t), E^*(t), I^*(t), R^*(t))$ is derived, thereby establishing

$$S^*(t) = \frac{\pi - (\mu+\nu)E(t)}{\mu},$$

$$E^*(t) = \frac{(\gamma+\alpha+\mu)I(t) - \theta R}{\nu},$$

$$I^*(t) = \frac{(\mu+\nu)(\mu+\theta)(\gamma+\alpha+\mu) - \beta S(t)\nu(\mu+\theta) - \theta\gamma(\mu+\nu)}{\theta\gamma(\mu+\nu) - \eta(\mu+\gamma)(\mu+\theta)(\gamma+\alpha+\mu)},$$

$$R^*(t) = \frac{\gamma I(t)}{\mu+\theta}.$$

3.3 LOCAL STABILITY

The local stability characteristics are determined by linearizing the model at the fixed point and generating the Jacobian matrix and the characteristic equation. The Jacobian matrix of the system of equations (1), specifically

$$J = \begin{bmatrix} -\frac{\beta I(t)}{1+\eta I(t)} - \mu & 0 & -\frac{\beta S(t)}{\left(1+\eta I(t)\right)^2} & 0 \\ \frac{\beta I(t)}{1+\eta I(t)} & -(\mu+\nu) & \frac{\beta S(t)}{\left(1+\eta I(t)\right)^2} & 0 \\ 0 & \nu & -(\gamma+\alpha+\mu) & \theta \\ 0 & 0 & \gamma & -(\mu+\theta) \end{bmatrix}. \quad (15)$$

Based on (15), the Jacobian matrix for the disease-free equilibrium (DFE) $E_0 = \left(\frac{\pi}{\mu}, 0,0,0\right)$ is

$$J(E_0) = \begin{bmatrix} -\mu & 0 & -\frac{\beta\pi}{\mu} & 0 \\ 0 & -(\mu+\nu) & \frac{\beta\pi}{\mu} & 0 \\ 0 & \nu & -(\gamma+\alpha+\mu) & \theta \\ 0 & 0 & \gamma & -(\mu+\theta) \end{bmatrix}.$$

Using matrix partition, we develop the characteristic equation for $J(E_0)$, namely

$$(-\mu-\lambda)\left\{(-(\mu+\nu)-\lambda)\begin{vmatrix} -(\gamma+\alpha+\mu)-\lambda & \theta \\ \gamma & -(\mu+\theta)-\lambda \end{vmatrix} - \nu\begin{vmatrix} \frac{\beta\pi}{\nu} & 0 \\ \gamma & -(\mu+\theta)-\lambda \end{vmatrix}\right\} = 0.$$

By doing standard algebraic calculations, it is determined that the eigenvalue $\lambda_1 = -\mu$, while the other eigenvalues are derived from the roots of characteristic equation:

$$\lambda^3 + A_1\lambda^2 + A_2\lambda + A_3 = 0,$$

with

$A_1 = 3\mu + \nu + \gamma + \alpha + \theta > 0$

$A_2 = (\gamma+\alpha+\mu)(2\mu+\nu) + (\mu+\nu)(\mu+\theta) + \theta(\alpha+\mu) - \beta\pi$

$A_3 = (\mu+\nu)\{\mu(\gamma+\alpha+\mu) + \theta(\alpha+\mu)\} - \beta\pi(\mu+\theta).$

Based on the Routh-Hurwitz criteria, the disease-free equilibrium will be asymptotically stable if only if $A_1 > 0$, $A_3 > 0$, and $A_1A_2 - A_3 > 0$. According to the equation (15), we obtain the new form of Jacobian Matrix for disease endemic equilibrium (DEE), namely

$$J(E^*) = \begin{bmatrix} -\frac{\beta I^*}{1+\eta I^*} - \mu & 0 & -\frac{\beta S^*}{(1+\eta I^*)^2} & 0 \\ \frac{\beta I^*}{1+\eta I^*} & -(\mu+\nu) & \frac{\beta S^*}{(1+\eta I^*)^2} & 0 \\ 0 & \nu & -(\gamma+\alpha+\mu) & \theta \\ 0 & 0 & \gamma & -(\mu+\theta) \end{bmatrix}.$$

By solving the following equation $|J(E^*) - \lambda I| = 0$, we get the characteristic equation $J(E^*)$ is

$$\lambda^4 + B_1\lambda^3 + B_2\lambda^2 + B_3\lambda + B_4 = 0,$$

with

$$B_1 = A + 4\mu + \nu + \gamma + \alpha + \theta$$

$$B_2 = (A + \mu)(\mu + \nu) + (A + 2\mu + \nu)(\gamma + \alpha + 2\mu + \theta) + (\gamma + \alpha + \mu)(\mu + \theta)$$

$$B_3 = (\gamma + \alpha + 2\mu + \theta)(A + \mu)(\mu + \nu) + (A + 2\mu + \nu)(\gamma + \alpha + \mu)(\mu + \theta) + \nu B(1 + A)$$

$$B_4 = (A + \mu)(\mu + \nu)(\gamma + \alpha + \mu)(\mu + \theta) + \nu B(\mu + \theta)(1 + A)$$

$$A = \frac{\beta I^*}{1 + \eta I^*}$$

$$B = \frac{\beta S^*}{(1 + \eta I^*)^2}.$$

By taking the Routh-Hurwitz criteria, the endemic equilibrium become asymptotically stable if only if $B_1 > 0, B_4 > 0, B_1 B_2 - B_3 > 0$, and $B_1 B_2 B_3 - B_3^2 - B_1^2 B_4 > 0$.

4. OPTIMAL CONTROL PROBLEMS

Optimization of model (1) through the application of control variables $\psi_1(t)$ aims to minimize interactions between susceptible and infected populations, while $\psi_2(t)$ represents a control strategy that includes administering treatment to the infected population. Consequently, model (1), which includes control variables, can be expressed in the following system of equations.

$$\begin{aligned}
\frac{dS(t)}{dt} &= \pi - \frac{\big(1 - \psi_1(t)\big)\beta S(t) I(t)}{1 + \eta I(t)} - \mu S(t) \\
\frac{dE(t)}{dt} &= \frac{\big(1 - \psi_1(t)\big)\beta S(t) I(t)}{1 + \eta I(t)} - (\mu + \nu) E(t) \\
\frac{dI(t)}{dt} &= \nu E(t) - (\gamma + \alpha + \mu) I(t) + \theta R(t) - \psi_2(t) I(t) \\
\frac{dR(t)}{dt} &= \gamma I(t) - (\mu + \theta) R(t).
\end{aligned} \tag{16}$$

The objective of optimal control is to achieve the optimal value condition for the model (16). In this section, we establish an optimum control criterion to minimize the objective function, such that

$$J\big(\psi_1(t), \psi_2(t)\big) = \int_{t_0}^{t_f} \left(E(t) + I(t) + \frac{1}{2}\psi_1^2(t) + \frac{1}{2}\psi_2^2(t) \right) dt. \tag{17}$$

The coefficients $\frac{1}{2}$ indicate the effort necessary to implement the controls, using only positive parameters, we derive the best control $\psi_1^*(t)$ and $\psi_2^*(t)$ such that:

$$J\big(\psi_1^*(t),\psi_2^*(t)\big) = \min\big\{J\big(\psi_1(t),\psi_2(t)\big), \text{with } \psi_1(t),\psi_2(t) \in U\big\},$$

concerning the domain $U = \big\{\big(\psi_1(t),\psi_2(t)\big): 0 \le \psi_1(t) \le 1;\ 0 \le \psi_2(t) \le 1\big\}$. Pontryagin's Minimum Principle provides a criterion for optimal control. This approach transforms (16) - (17) into a Hamiltonian function, as seen below:

$$\begin{aligned} H = E(t) + I(t) + \frac{1}{2}\psi_1^2(t) + \frac{1}{2}\psi_2^2(t) \\ + \lambda_S\left(\pi - \frac{\big(1-\psi_1(t)\big)\beta S(t)I(t)}{1+\eta I(t)} - \mu S(t)\right) \\ + \lambda_E\left(\frac{\big(1-\psi_1(t)\big)\beta S(t)I(t)}{1+\eta I(t)} - (\mu+\nu)E(t)\right) \\ + \lambda_I(\nu E(t) - (\gamma+\alpha+\mu)I(t) + \theta R(t) - \psi_2(t)I(t)) \\ + \lambda_R\big(\gamma I(t) - (\mu+\theta)R(t)\big), \end{aligned} \tag{19}$$

where $\lambda_S, \lambda_E, \lambda_I, \lambda_R$ are the costate (adjoint) variables relevant for optimal control. Subsequently, the theorem of optimal control is established using Pontryagin's Minimum Principle, as expressed

Theorem 3. *If the variables $\psi_1^*(t), \psi_2^*(t)$ are present, and the combined solution of $S^*(t), E^*(t), I^*(t), R^*(t)$ is valid for system (16), which minimizes $J\big(\psi_1(t),\psi_2(t)\big)$ in region U. There are adjoint (costate) variables $\lambda_S, \lambda_E, \lambda_I, \lambda_R$, that satisfy the equations system*

$$\frac{d\lambda_S}{dt} = \lambda_S\left(\frac{\big(1-\psi_1(t)\big)\beta I(t)}{1+\eta I(t)} + \mu\right) - \lambda_E\left(\frac{\big(1-\psi_1(t)\big)\beta I(t)}{1+\eta I(t)}\right)$$

$$\frac{d\lambda_E}{dt} = -1 + \lambda_E(\mu+\nu) - \lambda_I(\nu)$$

$$\frac{d\lambda_I}{dt} = -1 + \lambda_S\left(\frac{\big(1-\psi_1(t)\big)\beta S(t)}{\big(1+\eta I(t)\big)^2}\right) - \lambda_E\left(\frac{\big(1-\psi_1(t)\big)\beta S(t)}{\big(1+\eta I(t)\big)^2}\right) + \lambda_I\big(\gamma+\alpha+\mu+\psi(t)\big) - \lambda_R\big(\gamma+\psi(t)\big)$$

$$\frac{d\lambda_R}{dt} = -\lambda_I(\theta) + \lambda_R(\mu+\theta).$$

Subsequently, include the transversality criterion $\lambda_S(t_f) = \lambda_E(t_f) = \lambda_I(t_f) = \lambda_R(t_f) = 0$, such as the set of optimal control variable $\psi_1^*(t), \psi_2^*(t)$ are

$$\psi_1^*(t) = min\left\{max\left(0, \frac{(\lambda_E - \lambda_S)\beta S_1(t) I_1(t)}{1 + \eta I(t)}\right), 1\right\}$$

$$\psi_2^*(t) = min\{max(0, (\lambda_I - \lambda_R) I(t)), 1\}.$$

Proof: The existence of an optimum control issue can possibly be established by using Pontryagin's Minimum Principle [8], [24]. Following that, the adjoint variables are obtained by differentiating the Hamiltonian function with respect to the state variable, and the system can be readily identified as bellows

$$\frac{d\lambda_S}{dt} = \lambda_S\left(\frac{(1 - \psi_1(t))\beta I(t)}{1 + \eta I(t)} + \mu\right) - \lambda_E\left(\frac{(1 - \psi_1(t))\beta I(t)}{1 + \eta I(t)}\right)$$

$$\frac{d\lambda_E}{dt} = -1 + \lambda_E(\mu + \nu) - \lambda_I(\nu)$$

$$\frac{d\lambda_I}{dt} = -1 + \lambda_S\left(\frac{(1 - \psi_1(t))\beta S(t)}{(1 + \eta I(t))^2}\right) - \lambda_E\left(\frac{(1 - \psi_1(t))\beta S(t)}{(1 + \eta I(t))^2}\right) + \lambda_I(\gamma + \alpha + \mu + \psi(t)) - \lambda_R(\gamma + \psi(t))$$

$$\frac{d\lambda_R}{dt} = -\lambda_I(\theta) + \lambda_R(\mu + \theta).$$

by using the transversality criteria $\lambda_S(t_f) = \lambda_E(t_f) = \lambda_I(t_f) = \lambda_R(t_f) = 0$. The following section outlines how an optimum control variable may be determined by differentiating the Hamiltonian function with respect to the control $\psi_1(t), \psi_2(t)$, and assessing the outcome as zero, we get the control values as

$$\psi_1^*(t) = min\left\{max\left(0, \frac{(\lambda_E - \lambda_S)\beta S_1(t) I_1(t)}{1 + \eta I(t)}\right), 1\right\}$$

$$\psi_2^*(t) = min\{max(0, (\lambda_I - \lambda_R) I(t)), 1\}.$$

5. NUMERICAL RESULTS

5.1 FITTING PARAMETERS

By detecting Tuberculosis cases in Malang City, data was gathered through analysis of susceptible and infected people from 2014 to 2022.

Table 2. Tuberculosis Cases in Malang City

No	Years	Susceptible	Infected
1	2014	7915	1433
2	2015	7525	1336
3	2016	8304	1854
4	2017	7982	1783
5	2018	8085	1835
6	2019	10654	1965
7	2020	8868	1316
8	2021	14393	1438
9	2022	19299	2216

Based on the data in table 2, we have fitted the parameters by using Genetic Algorithm (GA), and we get the estimate of all parameters for model (1) is shown in Table 3.

Table 3. Fitting Parameters Through GA

Parameters	Interpretation	Estimation
π	A recruitment rate of susceptible subpopulation	0.53268
β	The contact rate of susceptible with infected or exposed subpopulation	0.15658
η	The saturation rate of infection	0.85823
μ	The natural mortality rate	0.25967
ν	The rate of exposed become infected subpopulation	0.91502
α	The mortality cause infection	0.10563
γ	Recovery rate	0.25163
θ	Reinfection rate	0.6496

5.2 DETERMINISTIC MODEL RESULT

To validate and elaborate the analytical findings of the previously established model (1). Utilizing the MATLAB 2021a software, we provide a numerical analysis of system (1). In this chapter, we establish the initial condition values as $S(0) = 10$, $E(0) = 5$, $I(0) = 2$, and $R(0) = 0$. Based on the parameter value in Table 3, we obtain the reproduction number of SEIR model Tuberculosis is $R_0 = \sqrt{\frac{\beta\pi\nu}{\mu(\mu+\nu)(\gamma+\alpha+\mu)}} = 2.2027 > 1$, and its indicates that the transmission of Tuberculosis is going to persist within a group of people.

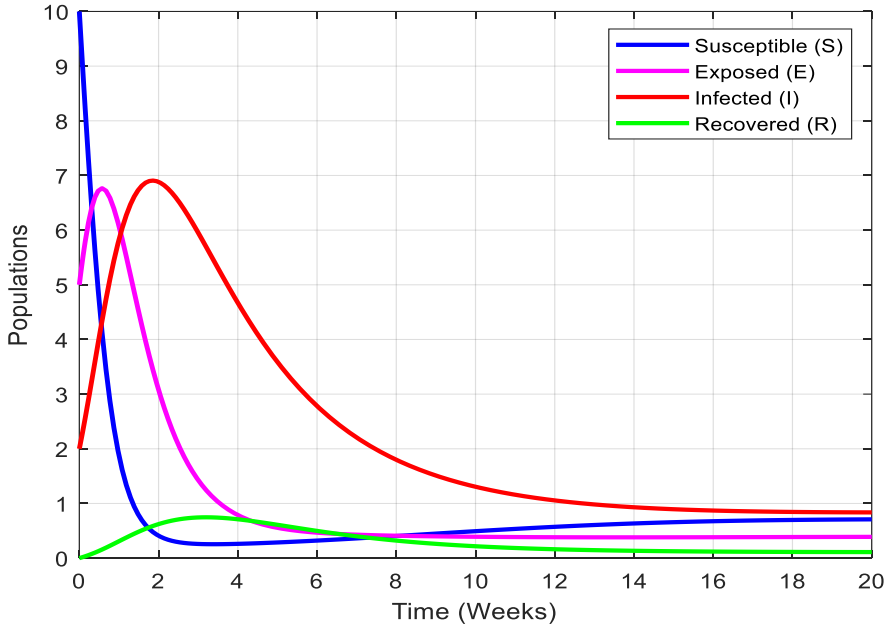

Figure 1. Dynamical Solution of Deterministic Model

Figure 1 illustrates a simulation of the SEIR epidemiological model, demonstrating the historical track of tuberculosis transmission. In the beginning, a larger section of the population was classified as susceptible; however, the proportion of susceptible people rapidly reduced as an increasing number of individuals became exposed and ultimately got the illness. During the interval between the second and third week, the occurrence of patients with infections peaked. As situations got worse an increasing number of persons recovered, which brought about a significant decrease in the infected population. Ultimately, between the 10th and 20th weeks, the population that was more sensitive and infected approached zero, meaning that most people had recovered

and acquired immunity, encourage confidence over the demise of disease transmission. A 3D simulation will demonstrate that all trajectories originating from five different initial values converge to a single fixed point. This signifies that the fixed point is stable.

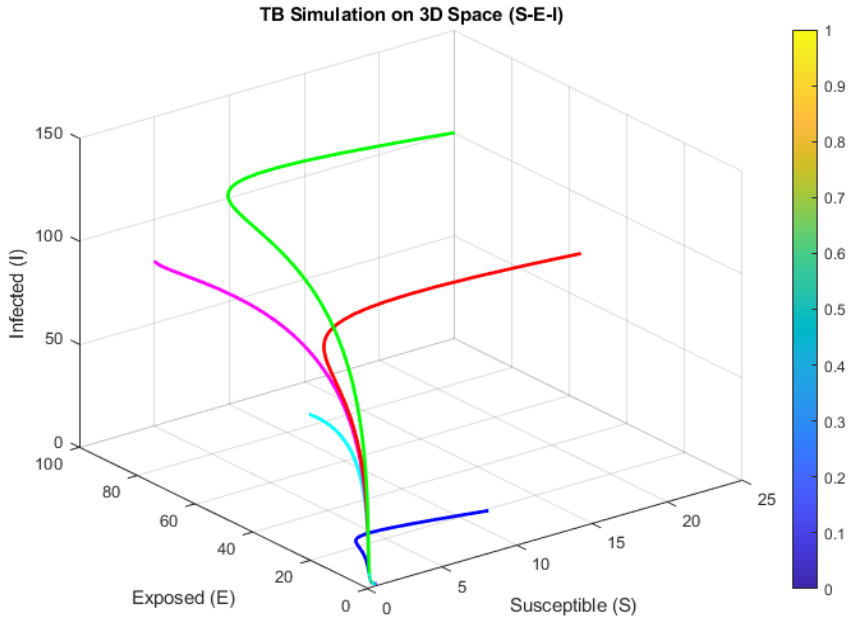

Figure 2. Phase Portrait on 3D Space $S - E - I$

According to figure (2), there are many curves present. The blue curve likely represents the trajectory with beginning values of $S = 10$, $E = 10$, and $I = 10$. Currently, the global incidence of the illness is not significant, with little change in the susceptible and exposed populations. The magenta curve probably signifies beginning values of $S = 5$, $E = 100$, and $I = 80$, suggesting a substantial rise in the exposed and infected populations. The simulation indicates an increased transmission of the disease from the first large population of exposed people. The green curve shows a significant peak in the infected population, indicating aggressive transmission, while the red curve shows a significant increase in the number of infections, indicating active spread despite a relatively smaller susceptible population. The last cyan curve illustrates that, despite the relatively small size of the susceptible group, the infection remains strikingly substantial among those previously exposed.

5.3 STOCHASTIC MODEL RESULT

This section will provide several simulations of stochastic models by applying different amounts of perturbation to evaluate the effects of disturbances on the Wiener process. Base on the equation system (2), and by taking the initial values are $S(0) = 10$, $E(0) = 5$, $I(0) = 2$, $R(0) = 0$, and all parameters in the Table 3.

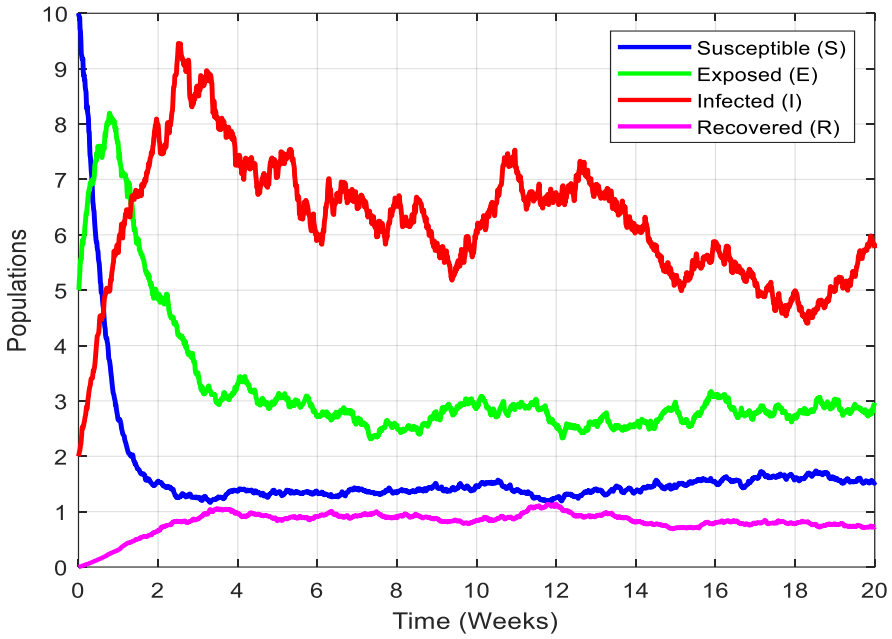

Figure 3. The Solution System (2) Using the Drift Values as $\sigma_S = \sigma_E = \sigma_I = \sigma_R = 0.1$.

The simulation presents a series of curves: the blue curve represents the group most susceptible to infection, the green curve identifies the exposed population, the red curve shows the infected population, and the magenta curve demonstrates the recovered population. The susceptible population at first declines due to being exposed, whereas the exposed population swiftly arrives at a peak, reflecting fluctuations linked to the model's stochastic properties. The diagnosed population shows considerable variability, contradicting deterministic models, due to uncertainty in transmission of disease and recovery. The recovered population gradually rises, with the total recoveries regularly growing; nevertheless, changes occur at more slowly than in other compartments. Moreover, the simulation will illustrate that an increase in the size of the applied disturbance correlates with a stronger effect on the model's fluctuations. For example, the drift values are taken as follows $\sigma_S = \sigma_E = \sigma_I = \sigma_R = 0.6$, we get the simulations bellow:

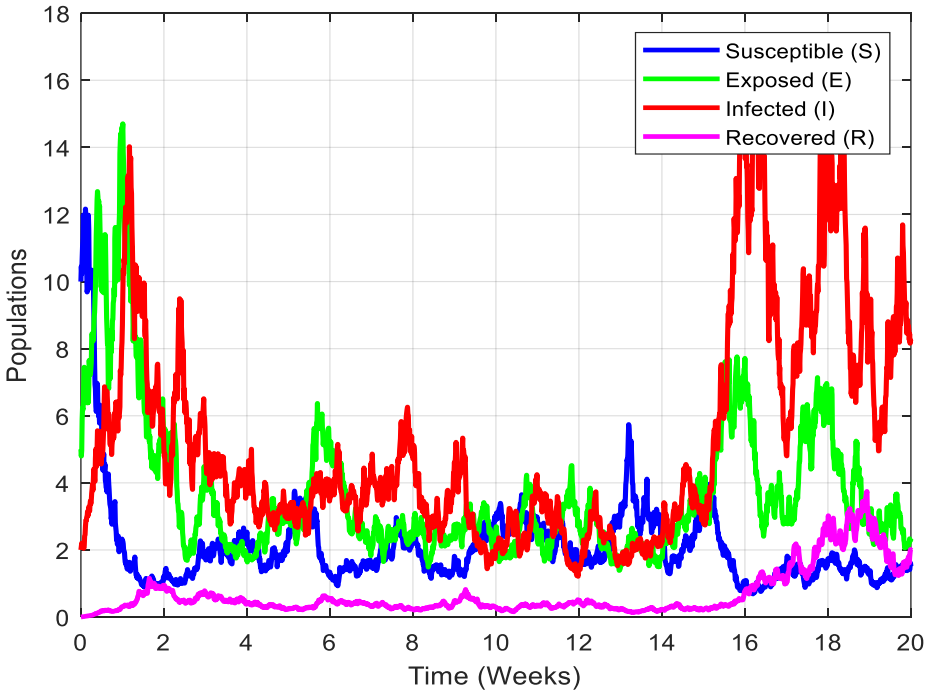

Figure 4. The Solution System (2) Using the Drift Values as $\sigma_S = \sigma_E = \sigma_I = \sigma_R = 0.6$.

Based on the figure (4), at the beginning of the simulation, it appears that there is a significant size of individuals in the Susceptible and Infected. Indicating an initial exposed population become illness. In the first few weeks, the number of individuals in the infected population increased drastically, followed by a decrease in the number of Susceptible. This state establishes the most acute form of disease transmission, characterized by a significant number of individuals being infected and experiencing illness. The quantity of Exposed fluctuates signifying a period of latency between being exposed and the beginning of disease. Subsequent to the acute period (about weeks 5 to 7), the number of Infected diminishes, whilst the population of Recovered increases. This indicates that several individuals have recovered from the illness and acquired immunity. Between weeks 15 and 20, there was a significant increase in the number of Infected and Exposed, indicating a second wave of the disease.

5.4 OPTIMAL CONTROL SIMULATIONS FOR DETERMINISTIC MODEL

To verify the analytical findings of the optimum control theorem previously discussed, we provide a numerical simulation of system (16) using the starting conditions $S(0) = 10$, $E(0) = 5$,

$I(0) = 2$, and $R(0) = 0$. Based on the numbers in Table 3, we proceed with the simulation of the optimum control issues outlined below.

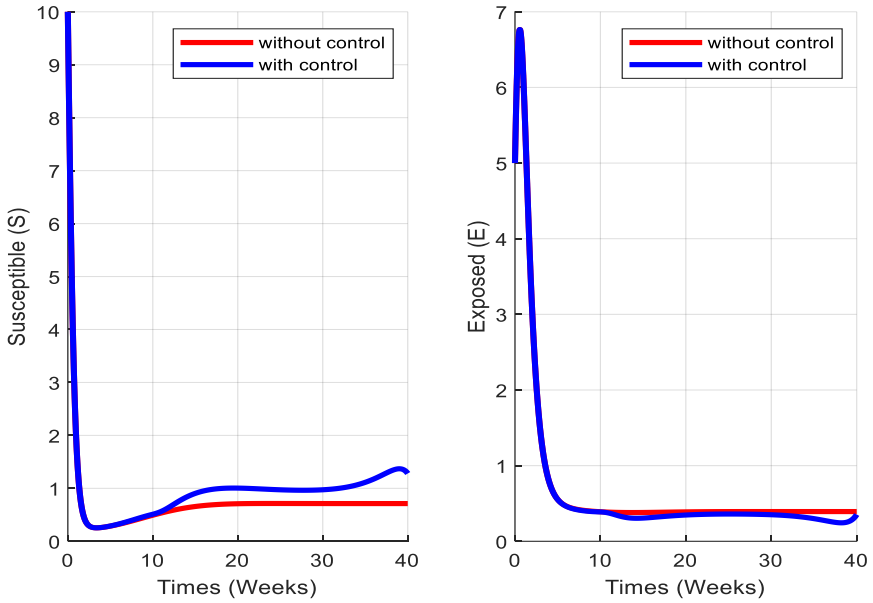

Figure 5. The Behavior Solutions of Susceptible and Exposed without and with control

Figure 5 depicts the modelling of tuberculosis (TB) transmission by comparing a scenario without intervention (red line) and another with established control measures. Cyan stripe. The first curve depicting the Susceptible population shows a quick decline in the beginning, especially in the uncontrolled scenario, when the virus spreads swiftly among people. This exposes several susceptible individuals to rapid infection. In the controlled scenario, the lowering of the Susceptible population occurs rapidly at first, then slows down by the 10th time point. This suggests that control measures might delay the spread of disease. The second graph depicts a rapid rise in the Exposed population initially, then by decreasing trend until a stable level is obtained. Nevertheless, the simulation results demonstrate that the solution dynamics, both with and without control, show little variation. The way of controlling interactions between those who are susceptible and those who are infected does not significantly reduce the infected population.

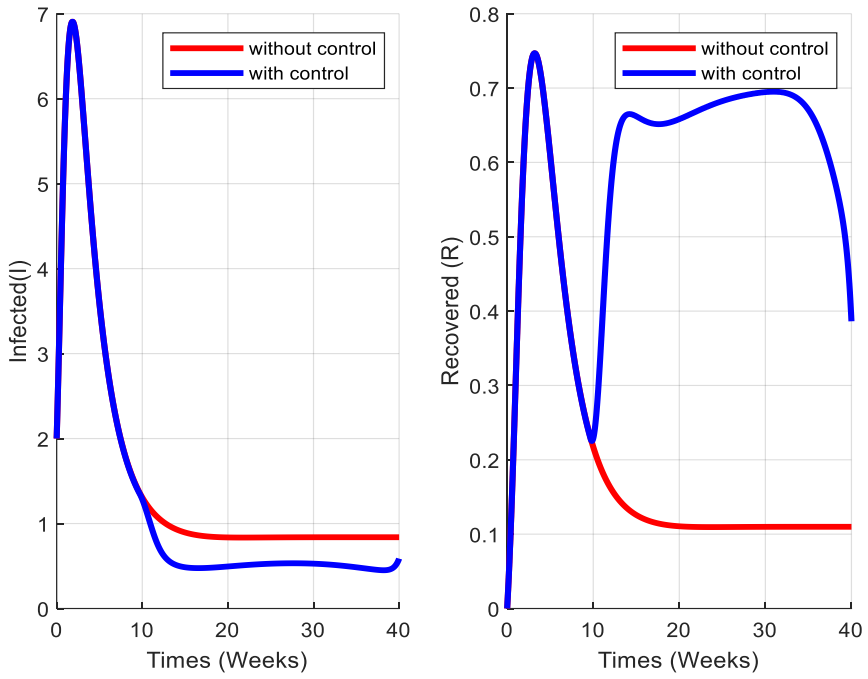

Figure 6. The Behavior Solutions of Infected and Recovered without and with control

On the left side of the graph in Figure 6 is a representation of the number of people infected with TB. In the uncontrolled scenario, the number of infected individuals increases quickly in the first week, after that declines gradually, and stable at a low level by the tenth week. Alternatively, under the controlled setting, the starting infection count is higher; nevertheless, the decline occurs more rapidly, reaching a very low value by around the fifteenth week. This indicates that control measures may accelerate the decrease of impacted individuals. The graph on the right illustrates the number of individuals recovering from TB infection. The uncontrolled scenario shows a slow recovery rate, as the number of patients recuperating remains continuously low and stable until week 40. In contrast, inside the controlled environment, the recovery rate of individuals rapidly increased throughout the first phase, reaching a peak of 0.7 between weeks 15 and 20. In contrast to the uncontrolled scenario, it maintained a greater level despite a little following decline. This suggests that, under supervision, several individuals were able to recover in a short timeframe.

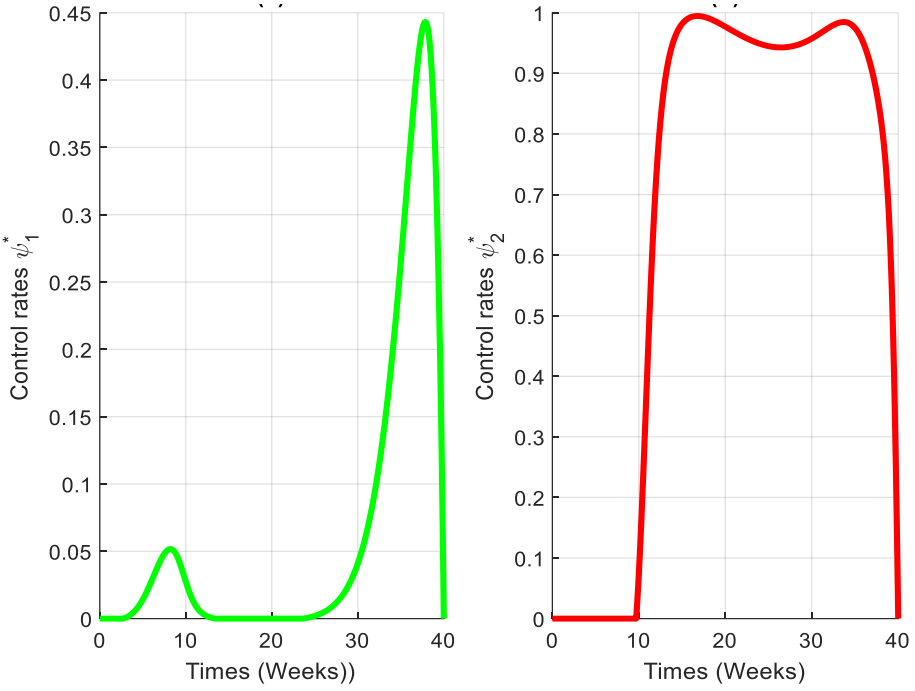

Figure 7. The Dynamical Control Rates ψ_1 and ψ_2

Figure 7 describes the trajectory of the solution for the two control variables $\psi_1(t)$ and $\psi_2(t)$ using an interval of 40 weeks, with the goal of regulating the spread of tuberculosis. The left graph indicates that control $\psi_1(t)$ begins to activate about the first week, on the other hand, and with a little increase around the 10-th week. At the end of the simulation period, variable $\psi_1(t)$ rises around the 35-th week before decreasing. This shows that control $\psi_1(t)$ was increased at the end to prevent late infection spread. However, the right graph for control $\psi_2(t)$ shows a unique trend: it was immediately maximum level and maintained at high intensity until week 35. It represents that control $\psi_2(t)$ is the main intervention for long-term infection management, while control $\psi_1(t)$ is integrated at the end to guard against TB disease.

6. CONCLUSION

This paper discusses a mathematical model of Tuberculosis with saturated infection. This model is divided into four subpopulations: susceptible, exposed, infected, and recovered. Next, the model is constructed in the form of a deterministic differential equation. Based on the deterministic

model, two equilibrium points are obtained, namely the disease-free equilibrium and the endemic equilibrium. The stability of equilibrium was analyzed using the Routh-Hurwitz criterion. Then, a deterministic model was constructed involving two control variables, and the analysis results showed that the applied control variables exist. Finally, involved numerical simulations to support the analysis previously. Based on TB infection case data 2014-2022 in Malang, parameters implemented in the model were estimated using the Genetic Algorithm method. The simulation results show that the deterministic model show smoothly curve and the persist of a pandemic. The stochastic model simulation shows that the noise variable significantly affects the fluctuations on the solution dynamics. When the noise value is high, it causes the model solution to experience sharper fluctuations. Last simulation of the optimal control problem shows that the applied control variables are capable of reducing the latent and infected populations. However, the treatment control variable is more effective $(\psi_1(t))$ than reducing interactions between populations $(\psi_2(t))$.

ACKNOWLEDGEMENT

This research is funded by the Ministry of Research and Higher Education of the Republic of Indonesia through the PDP program, under contract number 109/E.5/P.G.02.00.PL/2024.

CONFLICT OF INTEREST

The authors declare that there is no conflict of interest.

REFERENCES

[1] Y.A. Adi, Suparman, An investigation of Susceptible–Exposed–Infectious–Recovered (SEIR) tuberculosis model dynamics with pseudo-recovery and psychological effect, Healthc. Anal. 6 (2024), 100361. https://doi.org/10.1016/j.health.2024.100361.

[2] World Health Organization, Global Tuberculosis Report 2023, 2023.

[3] K.K. Avilov, A.A. Romanyukha, E.M. Belilovsky, S.E. Borisov, Mathematical modelling of the progression of active tuberculosis: Insights from fluorography data, Infect. Dis. Model. 7 (2022), 374–386. https://doi.org/10.1016/j.idm.2022.06.007.

[4] Dinkes Kota Malang, Profil kesehatan kota Malang tahun 2022, Malang, 2023.

[5] I.C. Eli, A.B. Okrinya, Sensitivity and stability analysis of tuberculosis disease with infectious latent, Int. J. Math. Stat. Stud. 11 (2023), 11–26. https://doi.org/10.37745/ijmss.13/vol11n31126.

[6] L. Hakim, L. Widayanti, Boundedness and existence analysis solution of an optimal control problems on mathematical COVID-19 model, BAREKENG J. Ilmu Mat. Terapan 18 (2024), 0797–0808. https://doi.org/10.30598/barekengvol18iss2pp0797-0808.

[7] L. Hakim, A.R. Habibi, Dynamic behavior of predator-prey with ratio dependent, refuge in prey and harvest from predator, ZERO J. Sains Mat. Terapan 3 (2019), 23. https://doi.org/10.30829/zero.v3i1.5886.

[8] S. Lenhart, J.T. Workman, Optimal control applied to biological models, Chapman and Hall/CRC, 2007. https://doi.org/10.1201/9781420011418.

[9] L. Hakim, A.R. Habibi, Perbandingan skema numerik metode finite difference dan spectral, J. Ilm. Tek. Inf. Asia, 10 (2016), 34–40.

[10] M.M. Ojo, O.J. Peter, E.F.D. Goufo, H.S. Panigoro, F.A. Oguntolu, Mathematical model for control of tuberculosis epidemiology, J. Appl. Math. Comput. 69 (2023), 69–87. https://doi.org/10.1007/s12190-022-01734-x.

[11] U.Y. Madaki, A.-A. Usman, A.E. Eghosa Elijah, A. Abdullahi, A mathematical modelling on tuberculosis dynamics incorporating treatment (A case study of General Hospital Potiskum, Yobe State), Scholars J. Phys. Math. Stat. 7 (2020), 240–259. https://doi.org/10.36347/sjpms.2020.v07i10.003.

[12] Y. Ucakan, S. Gulen, K. Koklu, Analysing of tuberculosis in turkey through SIR, SEIR and BSEIR mathematical models, Math. Computer Model. Dyn. Syst. 27 (2021), 179–202. https://doi.org/10.1080/13873954.2021.1881560.

[13] K.G. Mekonen, S.F. Balcha, L.L. Obsu, A. Hassen, Mathematical modeling and analysis of TB and COVID-19 coinfection, J. Appl. Math. 2022 (2022), 2449710. https://doi.org/10.1155/2022/2449710.

[14] F. Inayaturohmat, N. Anggriani, A.K. Supriatna, A mathematical model of tuberculosis and COVID-19 coinfection with the effect of isolation and treatment, Front. Appl. Math. Stat. 8 (2022), 958081. https://doi.org/10.3389/fams.2022.958081.

[15] F. Sulayman, F.A. Abdullah, Dynamical behaviour of a modified tuberculosis model with impact of public health education and hospital treatment, Axioms 11 (2022), 723. https://doi.org/10.3390/axioms11120723.

[16] M.A. Kuddus, E.S. McBryde, A.I. Adekunle, et al. Mathematical analysis of a two-strain tuberculosis model in Bangladesh, Sci. Rep. 12 (2022), 3634. https://doi.org/10.1038/s41598-022-07536-2.

[17] K. Oshinubi, O.J. Peter, E. Addai, et al. Mathematical modelling of tuberculosis outbreak in an East African country incorporating vaccination and treatment, Computation 11 (2023), 143. https://doi.org/10.3390/computation11070143.

[18] Y. Xue, X. Ruan, Y. Xiao, Measles dynamics on network models with optimal control strategies, Adv. Differ.

Equ. 2021 (2021), 138. https://doi.org/10.1186/s13662-021-03306-y.

[19] L. Hakim, Strategi kontrol optimal model SIQR pada penyebaran penyakit campak, Leibniz J. Mat. 2 (2022), 65–76. https://doi.org/10.59632/leibniz.v2i2.177..

[20] L. Hakim, Multiple strategies as optimal control of a COVID-19 disease with quarantine and using health masks, BAREKENG J. Ilmu Mat. Terapan 16 (2022), 1059–1068. https://doi.org/10.30598/barekengvol16iss3pp1059-1068.

[21] T.D. Keno, H.T. Etana, Optimal control strategies of COVID-19 dynamics model, J. Math. 2023 (2023), 2050684. https://doi.org/10.1155/2023/2050684.

[22] L. Hakim, A Pontryagin principle and optimal control of spreading COVID-19 with vaccination and quarantine subtype, Commun. Math. Biol. Neurosci. 2023 (2023), 94. https://doi.org/10.28919/cmbn/8157.

[23] C.E. Madubueze, K.A. Tijani, Fatmawati, A deterministic mathematical model for optimal control of diphtheria disease with booster vaccination, Healthc. Anal. 4 (2023), 100281. https://doi.org/10.1016/j.health.2023.100281.

[24] L. Hakim, T. Trisilowati, I. Darti, Optimal control of a cholera desease model with vaccination, Int. J. Appl. Math. Stat. 53 (2015), 65–72.

[25] M. Igoe, R. Casagrandi, M. Gatto, et al. Reframing optimal control problems for infectious disease management in low-income countries, Bull. Math. Biol. 85 (2023), 31. https://doi.org/10.1007/s11538-023-01137-4.

[26] S. Ullah, O. Ullah, M.A. Khan, T. Gul, Optimal control analysis of tuberculosis (TB) with vaccination and treatment, Eur. Phys. J. Plus 135 (2020), 602. https://doi.org/10.1140/epjp/s13360-020-00615-1.

[27] E. D.A.Ginting, D. Aldila, I.H. Febiriana, A deterministic compartment model for analyzing tuberculosis dynamics considering vaccination and reinfection, Healthc. Anal. 5 (2024), 100341. https://doi.org/10.1016/j.health.2024.100341.

[28] R.F. Appiah, Z. Jin, J. Yang, et al. Optimal control and cost-effectiveness analysis for a tuberculosis vaccination model with two latent classes, Model. Earth Syst. Environ. (2024). https://doi.org/10.1007/s40808-024-02128-7.

[29] Z. Ma, J. Li, J. Li, et al. Dynamical modeling and analysis of epidemics, World Scientific, 2009.